Geochemistry Geophysics Geosystems G3
AN ELECTRONIC JOURNAL OF THE EARTH SCIENCES
Published by AGU and the Geochemical Society

Article
Volume 10, Number 2
25 February 2009
Q02014, doi:10.1029/2008GC002149
ISSN: 1525-2027

GRACE gravity evidence for an impact basin in Wilkes Land, Antarctica

Ralph R. B. von Frese
School of Earth Sciences, Byrd Polar Research Center, Ohio State University, Columbus, Ohio 43210, USA

Laboratory for Space Geodesy and Remote Sensing Research, Ohio State University, Columbus, Ohio 43210, USA (vonfrese@geology.ohio-state.edu)

Laramie V. Potts
Department of Engineering Technology, New Jersey Institute of Technology, 2101 Guttenberg Information Technologies Center, University Heights, Newark, New Jersey 07102, USA

Laboratory for Space Geodesy and Remote Sensing Research, Ohio State University, Columbus, Ohio 43210, USA

Stuart B. Wells and Timothy E. Leftwich
School of Earth Sciences, Byrd Polar Research Center, Ohio State University, Columbus, Ohio 43210, USA

Laboratory for Space Geodesy and Remote Sensing Research, Ohio State University, Columbus, Ohio 43210, USA

Hyung Rae Kim
Department of Geoenvironmental Science, Kongju National University, 182 Shinkwan-dong, Gongju, ChungNam-do, 314-701, South Korea

Goddard Earth Sciences and Technology Center, University of Maryland Baltimore County, 5523 Research Park Drive, Suite 320, Baltimore, Maryland 21228, USA

Jeong Woo Kim
Department of Geomatics Engineering, University of Calgary, Calgary, Alberta T2N 1N4, Canada

School of Earth Sciences, Byrd Polar Research Center, Ohio State University, Columbus, Ohio 43210, USA

Alexander V. Golynsky
Department of Antarctic Geology, VNIIOkeangeologia, 1 Angliysky Avenue, St. Petersburg, 190121, Russia

Orlando Hernandez
Department of Geosciences, Universidad Nacional de Colombia, Carrera 30 No 45-03 Z.P. 06, Bogotá, Colombia

School of Earth Sciences, Byrd Polar Research Center, Ohio State University, Columbus, Ohio 43210, USA

Luis R. Gaya-Piqué
Equipe De Géomagnétisme, IPGS, CNRS, 2 place Jussieu, tour 14, F-75005 Paris, France

School of Earth Sciences, Byrd Polar Research Center, Ohio State University, Columbus, Ohio 43210, USA

[1] New details on the east Antarctic gravity field from the Gravity Recovery and Climate Experiment (GRACE) mission reveal a prominent positive free-air gravity anomaly over a roughly 500-km diameter subglacial basin centered on (70°S, 120°E) in north central Wilkes Land. This regional inverse correlation

between topography and gravity is quantitatively consistent with thinned crust from a giant meteorite impact underlain by an isostatically disturbed mantle plug. The inferred impact crater is nearly three times the size of the Chicxulub crater and presumably formed before the Cretaceous formation of the east Antarctic coast that cuts the projected ring faults. It extensively thinned and disrupted the Wilkes Land crust where the Kerguelen hot spot and Gondwana rifting developed but left the adjacent Australian block relatively undisturbed. The micrometeorite and fossil evidence suggests that the impact may have occurred at the beginning of the greatest extinction of life on Earth at ~260 Ma when the Siberian Traps were effectively antipodal to it. Antipodal volcanism is common to large impact craters of the Moon and Mars and may also account for the antipodal relationships of essentially half of the Earth's large igneous provinces and hot spots. Thus, the impact may have triggered the "Great Dying" at the end of the Permian and contributed to the development of the hot spot that produced the Siberian Traps and now may underlie Iceland. The glacial ice up to a few kilometers thick that has covered the crater for the past 30–40 Ma poses formidable difficulties to sampling the subglacial geology. Thus, the most expedient and viable test of the prospective crater is to survey it for relevant airborne gravity and magnetic anomalies.

Components: 7856 words, 9 figures.

Keywords: megaimpact; GRACE; Antarctica.

Index Terms: 8136 Tectonophysics: Impact phenomena (5420, 6022); 8137 Tectonophysics: Hotspots, large igneous provinces, and flood basalt volcanism; 4207 Oceanography: General: Arctic and Antarctic oceanography (9310, 9315).

Received 2 July 2008; **Revised** 18 December 2008; **Accepted** 13 January 2009; **Published** 25 February 2009.

von Frese, R. R. B., L. V. Potts, S. B. Wells, T. E. Leftwich, H. R. Kim, J. W. Kim, A. V. Golynsky, O. Hernandez, and L. R. Gaya-Piqué (2009), GRACE gravity evidence for an impact basin in Wilkes Land, Antarctica, *Geochem. Geophys. Geosyst.*, *10*, Q02014, doi:10.1029/2008GC002149.

1. Introduction

[2] The cause of the greatest mass extinction of life on Earth at the end of the Permian is uncertain and poorly documented in the geologic record because of the paucity of conformable stratigraphic units that span the Permian-Triassic boundary. The "Great Dying" has been attributed to the development of the Siberian Traps at ~253 Ma into the largest continental volcanic province of the Phanerozoic [e.g., *Renne and Basu*, 1991]. However, chondritic meteorite fragments discovered in rocks of the Permian-Triassic boundary in Antarctica suggested that meteorite impact(s) may also have contributed [*Basu et al.*, 2003].

[3] This discovery also is in line with the notion that large igneous provinces and hot spots developed antipodally to giant impacts [e.g., *Hagstrum*, 2005; *Boslough et al.*, 1996] because the Siberian Traps were generally antipodal to Antarctic Gondwana at the end of the Permian. Thus, the discovery sparked the hunt for Antarctic Gondwana impact(s) that may have almost exterminated life on Earth.

[4] *Becker et al.* [2004] identified the Bedout High off the northwestern coast of Australia as the possible central uplift of a Late Permian impact structure roughly the size of the Chicxulub impact basin. However, subsequent interpretation of deep seismic reflection, refraction, and borehole data suggested that the Bedout High was uplifted Permian basement rock from two roughly orthogonal rifting episodes in the Paleozoic and Cretaceous [*Müller et al.*, 2005].

[5] In Antarctica, seawater and ancient (30–40 Ma) ice sheets up to several kilometers thick cover any ring faults, shocked minerals, shatter cones, and other crustal evidence of impacts that may be there. Furthermore, the harsh and remote Antarctic environment greatly restricts collecting geophysical observations of the crust. Airborne gravity and magnetic survey coverage, for example, is extremely limited in general and especially lacking in detailed, low-altitude, high-resolution helicopter observations like those that discovered the Chicxulub crater [*Penfield and Camargo-Zanoguera*, 1981].

[6] However, the Gravity Recovery and Climate Experiment (GRACE) mission is mapping new satellite-altitude details of the gravity field that can greatly improve our understanding of the Antarctic crust. The added anomaly detail being captured by the GRACE mission is clearly evident

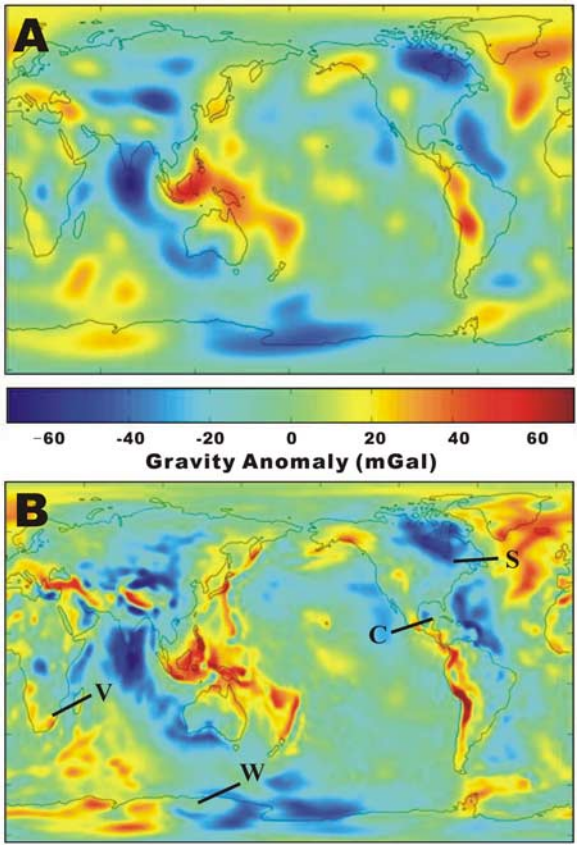

Figure 1. Comparison of the (a) pre-GRACE (i.e., EGM96) and (b) GRACE global gravity fields. Figure 1b also locates the Vredefort (V), Sudbury (S), Chicxulub (C), and putative Wilkes Land (W) craters.

by comparing the pre-GRACE gravity field from EGM96 [*Lemoine et al.*, 1998] in Figure 1a with the gravity field from GRACE [*Tapley et al.*, 2004] in Figure 1b.

[7] The GRACE observations are particularly valuable over Antarctica where surface gravity coverage is very poor [*von Frese et al.*, 1999; *Bell et al.*, 2002]. For the pre-GRACE Antarctic gravity field in Figure 1a, direct gravity constraints were essentially limited to satellite gravity observations at altitudes of about 1000 km and higher and satellite altimetry-derived gravity estimates from the adjacent southern oceans. The significantly more detailed Antarctic gravity field in Figure 1b from GRACE, on the other hand, reflects the direct mapping of gravity at altitudes of about 450 km across Antarctica.

[8] Over Wilkes Land (Figure 1b), in particular, GRACE mapped a circular, positive free-air gravity anomaly ringed by negative anomalies. Figure 2a presents this anomaly feature at 200 km elevation to enhance its spatial details. Figure 2b gives the related first vertical derivative anomaly that further isolates it from the regional gravity effects of the surrounding crustal components. These results center the anomaly on (70°S, 120°E) over the large subglacial basin in Figure 3 with the underlying circular region of thinned crust in Figure 4 that was derived from the modeled gravity effects of the basin's terrain.

[9] The eastern third of East Antarctica (Figure 3) from roughly 90°E longitude to the western margin of the Wilkes Subglacial Basin (WSB) includes the Gamburtsev Subglacial Mountains (GSM), Lake Vostok (LV), and numerous other possibly interconnected subglacial lakes [e.g., *Siegert*, 2000]. This relatively

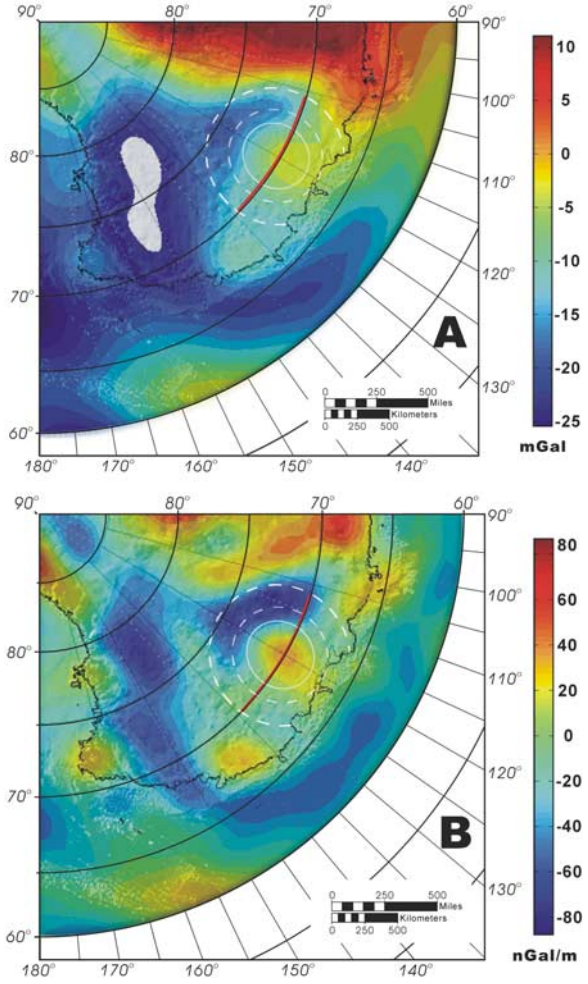

Figure 2. (a) GRACE satellite free-air gravity anomalies and (b) their first vertical derivatives at 200-km altitude. The white solid and dashed circles give the crustal rings inferred from the subglacial topography in Figure 3 and the "square root of 2 spacing rule," respectively [e.g., *Spudis*, 2005]. The bold red line shows the profile along 70°S considered in Figure 5.

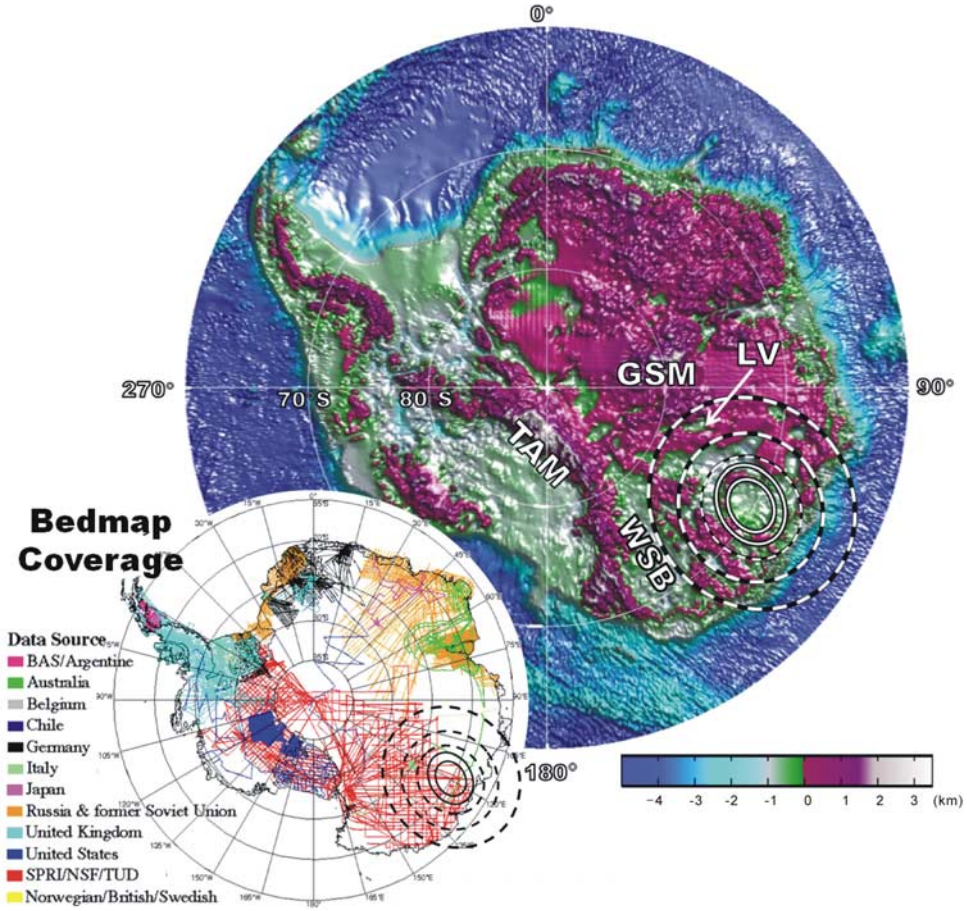

Figure 3. Antarctic BEDMAP bathymetry and subglacial topography (www.antarctica.ac.uk/mdms/meta_info/images/bedscr.gif). The central topographic ring of the inferred Wilkes Land impact crater is highlighted between two white solid circles and the dashed white circles highlight the partial ring structure according to the "square root of 2 spacing rule." Annotations include LV (Lake Vostok), GSM (Gamburtsev Subglacial Mountains), TAM (Transantarctic Mountains), and WSB (Wilkes Subglacial Basin). The inset shows the BEDMAP survey coverages.

broken up terrain has long been noted for its enigmatic crustal properties. Earthquake surface waves observed during the 1957–1958 International Geophysical Year (IGY) at the now-abandoned Wilkes Station (66°15′25.6″S, 110°31′32.2″E) first suggested that thinner-than-normal continental crust underlies as much as a quarter of the East Antarctic ice sheet [*Press and Dewart*, 1959]. Subsequent radio echo and seismic soundings of the ice sheet revealed the underlying regionally depressed subglacial topography in Figure 3 [*Drewry*, 1983a; *Lythe et al.*, 2001] that is compatible with the crustal thinning. Adjusting for the isostatic depression from the ice suggests that much of this topography may range over only ± 500 m, whereas isostatically adjusted elevations for the rest of East Antarctica would hold at about 1000–4000 m [*Drewry*, 1983b].

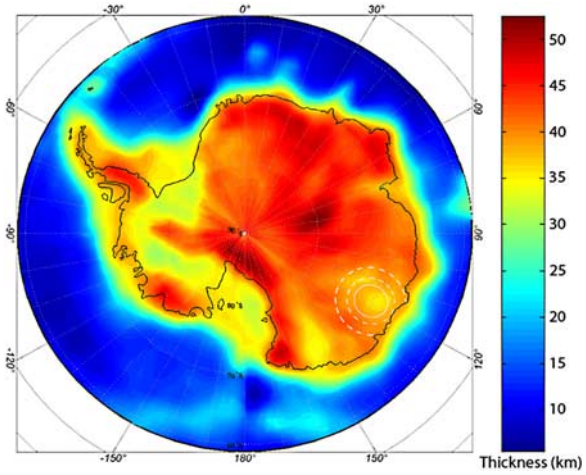

Figure 4. Antarctic crustal thickness map from *von Frese et al.* [1999] updated for the BEDMAP terrain data in Figure 3 and GRACE gravity observations [*Wells*, 2006].

[10] A pre-GRACE analysis of the depressed terrain's gravity effects indicated that the Moho here is roughly 7 km shallower than in the rest of East Antarctica [*von Frese et al.*, 1999]. This analysis involved computing the gravity effects of the ice, water, and rock components of the Antarctic terrain at a nominal satellite altitude (i.e., 150 km). From the correlation spectrum [*von Frese et al.*, 1997] between these effects and satellite-altitude free-air gravity anomalies, correlation filters were designed to extract positively and negatively correlated free-air components that were ascribed to isostatic imbalances of the crust [e.g., *von Frese et al.*, 1999; *Leftwich et al.*, 2005]. The Moho was modeled from the presumed isostatically balanced Bouguer anomalies obtained by subtracting the terrain gravity effects from the terrain-correlated free-air anomalies.

[11] This approach was also used to model crustal properties of large impact basins on the Moon [*von Frese et al.*, 1997; *Potts and von Frese*, 2003a, 2003b] and Mars [*Potts et al.*, 2004; *Leftwich*, 2006]. In addition, its validity was tested by mapping Moho variations of the Antarctic region south of 60°S [*von Frese et al.*, 1999], Iceland and the surrounding North Atlantic [*Leftwich et al.*, 2005], and Greenland [*Braun et al.*, 2007]. The gravity-derived Moho estimates in these regions were found generally to be well within 10% of the available seismic estimates.

[12] Another seismic model of the crust of Antarctica was developed by *Ritzwoller et al.* [2001] from an extensive set of fundamental mode surface wave dispersion measurements. Relative to the gravity modeling, the seismic analysis obtained a more regional crustal model that did not differentiate Antarctica's ice and rock terrain components. However, when the seismic model is adjusted for ice thickness variations, it broadly features crustal thinning in East Antarctica like that established by the pre-GRACE gravity analysis of *von Frese et al.* [1999].

[13] *Wells* [2006] updated the crustal thickness model of *von Frese et al.* [1999] for current terrain data [*Lythe et al.*, 2001] and the free-air gravity anomalies of the GRACE mission. These improved results shown in Figure 4 reveal a circular region of crustal thinning in Wilkes Land that is analogous to the crustal thinning effects observed for large impact craters on the Moon [e.g., *Spudis*, 2005; *Potts and von Frese*, 2003a, 2003b; *von Frese et al.*, 1997] and Mars [e.g., *Potts et al.*, 2004; *Neumann et al.*, 2004].

[14] In general, craters larger than about 300 km are called impact basins [e.g., *Spudis*, 2005]. Lunar and Martian impact basins are commonly overlain by ringed positive satellite gravity anomalies that may be attributed to the effects of uncompensated concentrations of mass produced within the crust from the impact [e.g., *Muller and Sjogren*, 1968; *Wise and Yates*, 1970; *von Frese et al.*, 1997; *Potts and von Frese*, 2003a, 2003b; *Potts et al.*, 2004]. The central anomaly peak is taken to reflect primarily the enhanced mass concentration or "mascon" of an uplifted, relatively dense mantle plug that was suspended in the crust when it recoiled from the meteorite impact. In the lunar craters, postimpact basaltic fill or mare also has been inferred to make additional minor contributions to the peak anomalies [e.g., *von Frese et al.*, 1997; *Potts and von Frese*, 2003a, 2003b].

[15] The flanking negative ring anomaly, on the other hand, can be readily interpreted as the effect of uncompensated crustal thickening around the margin of the impact basin [e.g., *von Frese et al.*, 1997; *Potts and von Frese*, 2003a, 2003b]. Thus, the strength of the lithosphere is presumed to maintain the higher density mascon (and mare fill if any) and the surrounding excessively thickened lower density crust against isostatic forces to produce the central positive and flanking negative ring anomalies, respectively.

[16] In the sections below, we quantitatively model the crustal properties of the inferred Wilkes Land impact basin from the GRACE data and terrain gravity effects. We also investigate the possible antipodal relationship between the Wilkes Land impact and the large igneous province of the Siberian Traps, as well as the implications of the inferred impact for the development of life on Earth, and the crustal properties and evolution of Wilkes Land and the conjugate tectonic block of Australia.

2. Gravity Anomaly Modeling

[17] The gravity anomaly estimates at 200-km altitude in Figure 2 were derived from the satellite-only GRACE gravity model [*Tapley et al.*, 2004] limited to spherical harmonic degree and order 90 to emphasize the more robust qualities of the actual GRACE measurements. The higher-frequency components (i.e., of degree and order >90) are relatively poorly determined according to the model's covariance properties. And at altitudes lower than 200 km, the anomaly estimates have

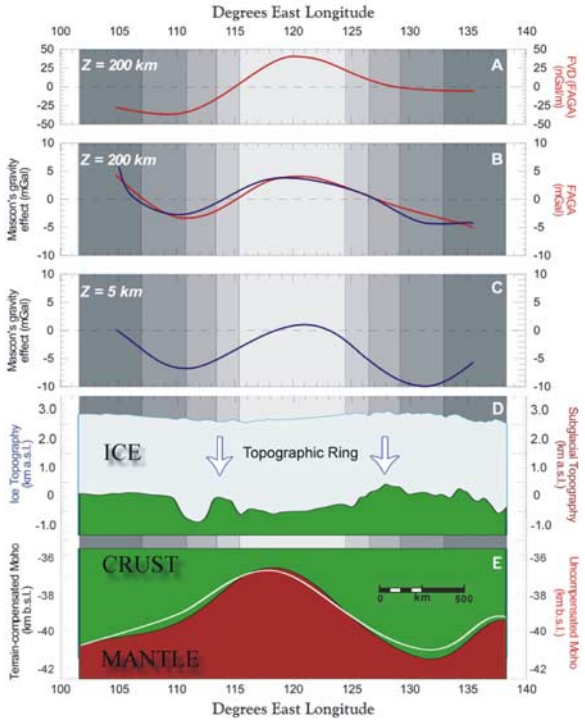

Figure 5. Crustal modeling along the 70°S profile segment highlighted in Figure 2 across the inferred Wilkes Land impact basin. (a) First vertical derivatives (FVD) of the (b) GRACE (red profile) free-air gravity anomalies (FAGA) at altitude Z = 200 km with the mean value of −4.83 mGals removed. The blue profile is the gravity effect of the mascon defined by the difference between the black and white Moho profiles in Figure 5e and the vertical gray shading delineates the projected rings across the profile. (c) Modeled mascon gravity effect at airborne altitude Z = 5 km. (d) Cross section of the ice and subglacial elevations that were modeled for their gravity effects at 200-km altitude. (e) Cross section of the lower crust and upper mantle where the black profile gives the Moho that accounts for the terrain's gravity effects at 200-km altitude. The white-lined Moho is the black-lined Moho adjusted to account for the GRACE free-air anomaly in Figure 5b.

dramatically increasing noise levels, as well as decreasing reliability due to the lack of terrestrial gravity observations [*von Frese et al.*, 1999] and the lack of uniqueness of the gravity modeling [*von Frese et al.*, 2005].

[18] The first vertical derivative gravity anomaly in Figure 2b enhances the details of the GRACE anomaly's strong spatial correlation with the inferred impact basin. The negative ring anomaly flanking the basin is relatively weak and broken up on the west but strongly expressed to the south. On the east, the signal is again weak due likely to the interfering gravity effects of crustal features related to the development of the Wilkes Subglacial Basin (WSB in Figure 3) west of the Transantarctic Mountains (TAM). On the northern margin, Cretaceous rifting apparently cut the flanking minimum.

[19] For the present study, we modeled the gravity effects of the terrain in spherical coordinates at 200 km altitude using Gauss-Legendre quadrature integration [*von Frese et al.*, 1981] and the respective densities of 0.90, 1.02, and 2.80 g/cm^3 for the ice, water, and rock components of the terrain. From the spectral correlation analysis of the terrain effects and GRACE data, terrain-correlated free-air components were estimated that included the mascon and flanking ring anomalies. We then modeled the isostatically balanced Bouguer anomalies for Moho variations assuming a 0.4 g/cm^3 density contrast between the mantle and crust.

[20] The crustal thickness values in Figure 4 were produced by subtracting the gravity-derived Moho estimates from the subglacial topographic and bathymetric elevations of BEDMAP. These three-dimensional Moho modeling results accommodate the GRACE data and gravity effects of the ice, water, and rock components of the BEDMAP terrain at 200 km altitude. They clearly show a prominent circular region of thinned crust beneath the large subglacial basin of Wilkes Land in Figure 3.

[21] These Moho estimates were fundamentally controlled by the gravity effects of the Antarctic terrain, which are large compared to the free-air anomalies [e.g., *von Frese et al.*, 1999]. Thus, adjusting the isostatically balanced Moho to also match the terrain-correlated free-air GRACE anomalies produced a slightly modified, isostatically imbalanced Moho where the differences between the two Moho levels account for the terrain-correlated free-air anomalies. These differences suggested that the mascon underlying the basin may involve roughly 0.8 km of uncompensated excess mantle plug relief, whereas the flanking negative ring anomaly can be accommodated by up to nearly 0.7 km of uncompensated excess crustal thickness around the plug. The modeling, although not unique, accounts for the massive, independently observed terrain and gravity data sets of the study region.

[22] Figure 5 summarizes our spherical three-dimensional modeling results along 70°S. In Figure 5e, the crust (green)-mantle (brown) interface is the isostatically imbalanced Moho inferred

from the gravity effects of the terrain in Figure 5d and the GRACE free-air anomalies (red) in Figure 5b, whereas the white profile gives the isostatically balanced Moho. The Moho difference at the central plug and its flanks has gravity effects given by the blue profile that match the GRACE data as shown in Figure 5b. These results characterize the mantle plug beneath the impact basin as being some 425 km across and 4–6 km thick. These vertical dimensions are probably minimal because erosion, sedimentation, and viscous relaxation of the crust have muted the subglacial topography.

3. Discussion

[23] Our analysis suggests that the terrain and GRACE gravity data can be explained by the crustal effects of a giant impact in Wilkes Land. Unfortunately, the geological details of the inferred impact site are completely masked by a few kilometers of overlying glacial ice. However, possible impact evidence has been reported from the Permian-Triassic boundary beds at Graphite Peak in the central Transantarctic Mountains (TAM). This evidence includes small chondritic meteorite fragments [*Basu et al.*, 2003], fullerenes with extraterrestrial noble gas abundances and isotope ratios [*Poreda and Becker*, 2003], and a faint iridium anomaly [*Retallack et al.*, 1998]. The strength of this evidence has been debated [e.g., *Collinson et al.*, 2006] and obviously limited by the apparent absence of a source crater. However, the putative crater clearly may be a source of the Graphite Peak data and thus may yield new insights on a possible late Permian impact origin for the great mass extinction. In view of its potential geological significance, we investigate below additional constraints on the possible crustal properties and evolution of the inferred Wilkes Land impact.

[24] The impact scenario, for example, helps to account for the enigmatic one-sided nature of the crustal thinning in East Antarctica relative to the normal thickness of the adjacent Australian crust [e.g., *Clitheroe et al.*, 2000] that the impact and rifting left largely intact. The apparent absence of this Australian effect is hardly diagnostic of impact age because it could have resulted from a large Antarctic impact anytime before or after the Cretaceous separation of Australia and East Antarctica. However, the possible crustal rings of the putative Wilkes Land impact suggest a minimum age that appears to exclude the younger impacts.

[25] In particular, large multiring basins of the Moon and other terrestrial planets tend to follow the "square root of 2 spacing rule" that estimates the diameter of the *n*th ring by $D_n = (\sqrt{2})^{n-1} \times D_1$ in terms of the central ring diameter, D_1 [e.g., *Spudis*, 2005]. Using $D_1 \approx 500$ km of the central ring inferred from the subglacial topography, the Wilkes Land coastline roughly intersects the northern margin of the second ring as shown in Figure 3.

[26] The coastline may have cut the second and wider rings because the rings do not appear to extend offshore in the satellite altimetry-derived marine gravity [*Marks and McAdoo*, 1992] and BEDMAP bathymetric estimates. The apparent crosscutting relationship suggests a minimum age constraint for the impact that accordingly would have occurred before the Cretaceous separation of the East Antarctic and Australian coastlines.

[27] As a crustal impact basin, the inferred Wilkes Land crater is unique for its great size and the fact that its mascon is the only one ever detected in the Earth's gravity field at satellite altitudes. The next largest impacts on record are the South African 300-km diameter, ~2.2 Ga Vredefort basin [e.g., *Carporzen et al.*, 2005] and the large Canadian 250-km diameter, ~1.85 Ga Sudbury crater (e.g., http://www.unb.ca/passc/ImpactDatabase/images/sudbury.htm). However, Figure 1b shows that these Precambrian craters do not appear to produce significant GRACE anomalies, presumably because they are essentially in isostatic equilibrium and their crustal dimensions are small compared to GRACE altitudes.

[28] The rest of the known impact craters of the Earth involve even smaller crustal disturbances that are simply too weak to give gravity signatures at GRACE altitudes. The famous 170-km diameter, 0.65 Ga Chicxulub crater in Mexico's Yucatán Peninsula, for example, yields a very well defined ringed positive gravity anomaly at airborne altitudes [*Penfield and Camargo-Zanoguera*, 1981], which Figure 1b suggests is essentially undetectable at GRACE altitudes. Thus, the crustal features of the craters in the Earth's current impact database derived from near-surface geologic and geophysical observations have very limited utility in accounting for the gravity effects of impact basins in the GRACE data.

[29] However, the gravity effects of the terrain and the GRACE free-air gravity observations over the inferred Wilkes Land impact crater are completely analogous with the terrain and satellite gravity data

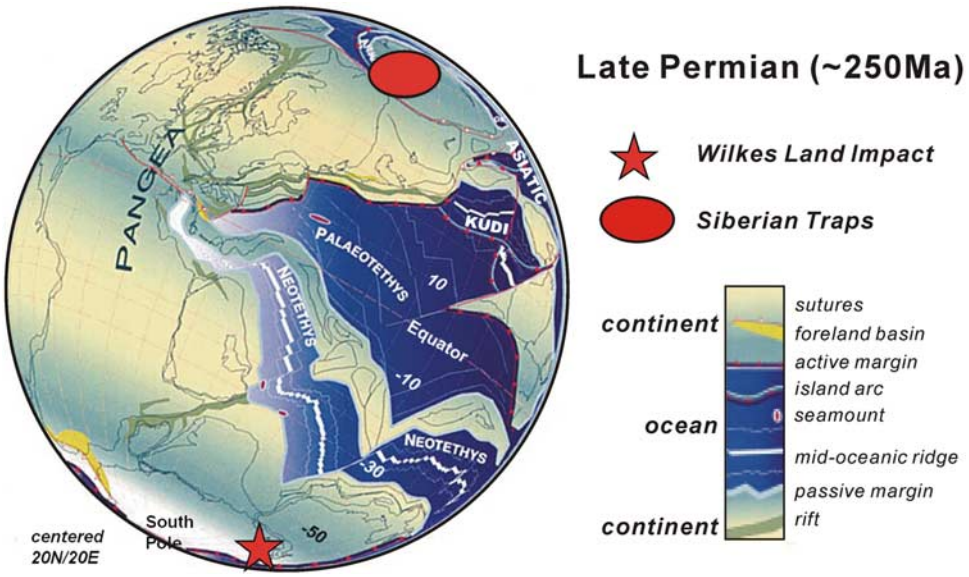

Figure 6. Possible antipodal relationship of the Wilkes Land impact and the Siberian Traps in the Late Permian continental reconstruction adapted from *Stampfli and Borel* [2002].

observed for the impact basins of the Moon [*von Frese et al.*, 1997; *Potts and von Frese*, 2003a, 2003b] and Mars [*Potts et al.*, 2004; *Leftwich*, 2006]. Exploiting these analogies is particularly appropriate because the more than 2-km thick ice sheet that covers the inferred Wilkes Land crater makes the geology nearly as inaccessible to direct sampling as it is for the lunar and Martian craters.

[30] Crustal disturbances at the antipodes of large impacts are common on the Moon [e.g., *Daily and Dyal*, 1979; *Schultz and Gault*, 1975; *Melosh*, 1989; *Spudis*, 2005; *Potts and von Frese*, 2003a, 2005; *Richmond et al.*, 2005], Mars [e.g., *Schultz and Glicken*, 1979; *Watts et al.*, 1991; *Reese et al.*, 2002; *Leftwich*, 2006], and the Earth [e.g., *Boslough et al.*, 1996; *Hagstrum*, 2005]. When considered in the context of a Late Permian impact as in Figure 6, the Wilkes Land basin also shows a striking antipodal relationship to the Siberian Traps. In reconstructed P-Tr coordinates [e.g., *Smith et al.*, 1981; *Stampfli and Borel*, 2002], the inferred antipode is within a 30° spherical cap centered on the Siberian Traps, which represents about 6% of the Earth's total surface area. The statistical significance of the antipodal relationship accordingly appears quite strong given the low probability for the antipode to have randomly fallen this close to the Siberian Traps.

[31] The apparent 15° misfit of the antipode is entirely in paleolongitude and may result from several little understood influences. Late Permian paleomagnetic data, for example, constrain paleolongitudes very poorly [e.g., *Smith et al.*, 1981], and an oblique impact offsets the antipode in the direction of the incoming trajectory [e.g., *Schultz*, 2007]. Antipodal energy also might excite volcanism at offset crustal faults, fractures, hot spots, and other preimpact structures.

[32] The possible antipodal relationship in Figure 6 may constrain the impact to some time before the onset of the greatest Phanerozoic continental volcanic activity at ~253 Ma. However, detailed stratigraphic studies of isolated sections in eastern Asia suggest that the P-Tr extinction involved two distinct events [e.g., *Isozaki*, 2004]. The Guadalupian-Lopingian extinction occurred first at roughly 260 Ma where up to 58% of marine genera disappeared [*Stanley and Yang*, 1994]. About 5–10 million years later, the main extinction followed with the disappearance of up to 90% of marine life and about 75% of the terrestrial vertebrates and the reduction of plant life mostly to the fungal stage [e.g., *Erwin*, 1994].

[33] The impact might then have occurred shortly before 260 Ma, but just when in the Late Wordian is difficult to say because our understanding of how giant impacts produce antipodal effects is limited. In general, postimpact volcanic materials are associated with major impact basins and antipodes [e.g., *Melosh*, 1989; *Spudis*, 2005], but the mechanisms by which this volcanism occurs millions to perhaps hundreds of millions of years after impact are very poorly understood [e.g., *Melosh*, 2000; *Jones et al.*, 2002; *Ivanov and Melosh*, 2003; *Melosh*, 2003a, 2003b]. Despite

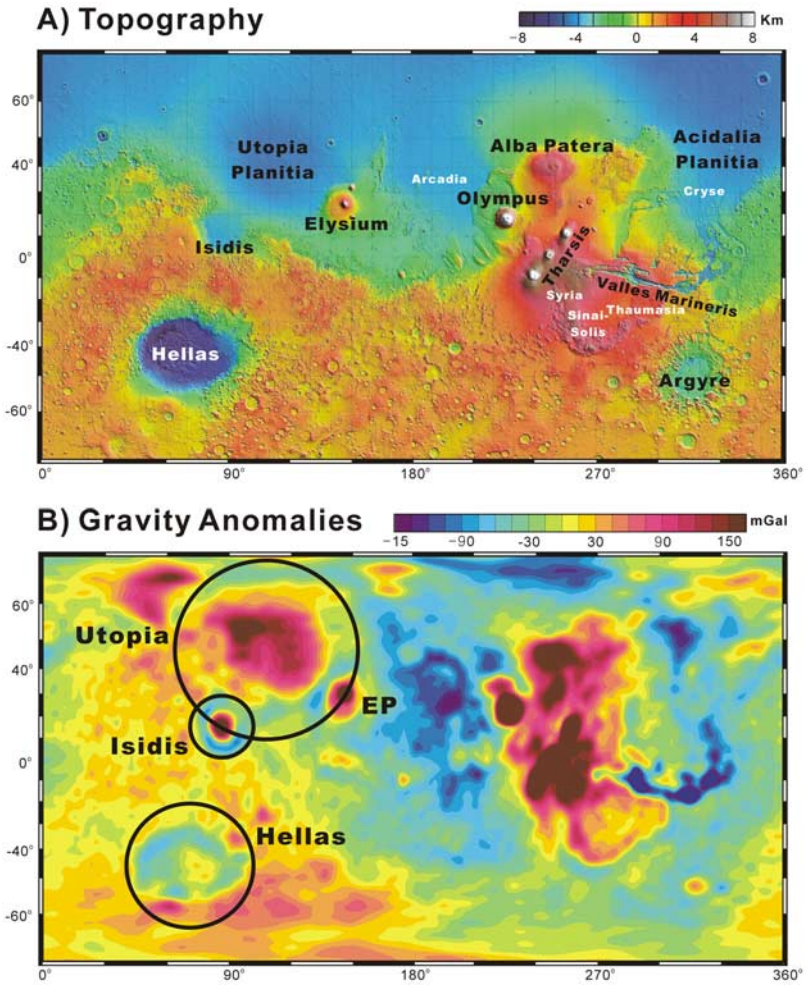

Figure 7. (a) Mars topography and (b) free-air gravity anomalies showing the characteristic gravity signatures for giant impacts and major volcanic provinces. The black circles broadly delineate the central basins for some giant impacts of the eastern hemisphere. The ringed positive gravity anomaly overlying the major Elysium Planitia (EP) volcanic province in Figure 7b is centered on Elysium Mons in Figure 7a.

these uncertainties, however, the evidence of substantial antipodal effects from giant impacts seems clear and abundant.

[34] On the Moon, for example, the antipodes of impact basins tend to exhibit grooved and disrupted terrain [e.g., *Schultz and Gault*, 1975; *Melosh*, 1989; *Spudis*, 2005; *Schultz*, 2007] and magnetic disturbances [e.g., *Daily and Dyal*, 1979; *Richmond et al.*, 2005] that strongly suggest the seismic focusing of impact energies. The lunar nearside basaltic maria are essentially antipodal to the great South Pole Aitken Basin where impact event effects may have extended to the lunar core [*Potts and von Frese*, 2003a, 2005].

[35] On Mars, the crustal associations between volcanic provinces and the impact basins and their antipodes are remarkably clear despite considerable impact gardening, and wind and water erosion of the crustal surface [e.g., *Barlow*, 1990; *Hartmann*, 1999; *Hartmann and Berman*, 2000; *Hartmann et al.*, 2001]. Figure 7a, for example, gives the crustal topography [*Smith et al.*, 1999a] from the Mars Orbital Laser Altimeter (MOLA), and Figure 7b the free-air gravity anomalies [*Smith et al.*, 1999b], which were both mapped by the Mars Global Surveyor (MGS) mission. The topography shows the eroded surfaces of several large basins with overlying central gravity maxima ringed by gravity minima at satellite altitude that mark these basins as impact craters.

[36] This gravity signature is not unique to impact basins but also marks volcanic provinces such as Elysium Planitia (EP in Figure 7b). However, the crustal thickness variations of Mars estimated by *Neumann et al.* [2004] from the MOLA terrain and gravity data in Figure 8 clearly differentiate the

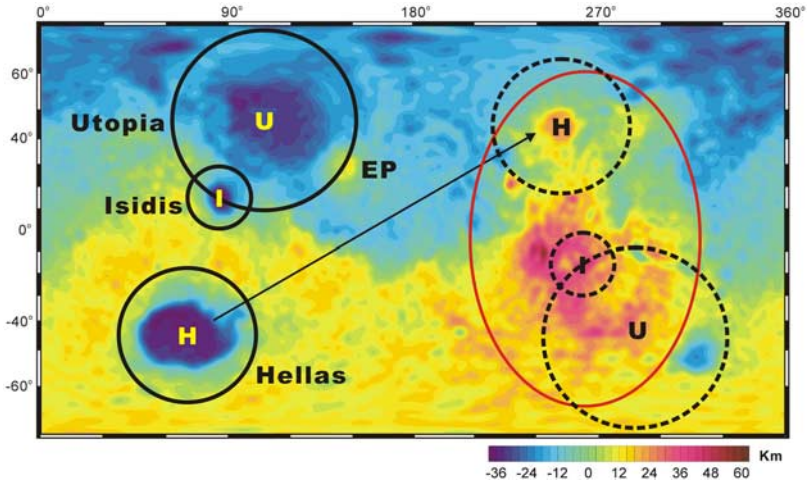

Figure 8. Martian crustal thickness variations differentiate the similar gravity anomalies of impact basins and major volcanic provinces like Elysium Planitia (EP in Figure 7) as thinned and thickened crustal features, respectively. These gravity-inferred crustal thickness estimates of *Neumann et al.* [2004] also illustrate the antipodal relationships between giant impacts and volcanic provinces.

impact basins and volcanic provinces as respectively thinned and thickened crustal features [*Neumann et al.*, 2004; *Potts et al.*, 2004; *Leftwich*, 2006]. In similar fashion, the Antarctic gravity-inferred crustal thickness variations in Figure 4 characterize the source of the GRACE anomaly as thinned, isostatically disturbed crust such as produced by large meteorite impact. Figure 4, which fundamentally models the gravity effects of the BEDMAP terrain with minor adjustments imposed by the free-air data, does not support a volcanic origin for the GRACE anomaly as some reports have suggested (M. Peplow, Does a giant crater lie beneath the Antarctic ice?, *Nature News*, doi:10.1038/news060529-11, 2006, http://www.nature.com/news/2006/060529/full/news060529-11.html).

[37] The Martian crustal thickness estimates in Figure 8 also strongly relate impact basins to antipodal volcanism [e.g., *Williams and Greeley*, 1994]. The antipodes of the great eastern basins of Utopia (U), Isidis (I), and Hellas (H), for example, are all within the red ellipse enclosing the Tharsis province, which is the largest known volcanic center in the solar system. Here, matching yellow and black alphabetic identifiers mark the respective centers and antipodes of these basins, whereas encompassing solid and dashed black circles broadly outline the basins at their respective centers and antipodal locations. As an example, the arrow points from the center of the Hellas basin to its antipode at Alba Patera.

[38] In general, the likelihood that all three of these antipodes would lie in the Tharsis province is slight given that the red ellipse includes only about 13% of the Martian surface. Thus, the synthesis of MGS terrain and gravity observations into the crustal thickness estimates of Mars in Figure 8 suggests a strong correlation between giant impacts and antipodal volcanism. They also differentiate the impact basins and volcanic provinces into respective crustal thinning and thickening events. Thus, these results provide a very useful perspective for considering the possible effects of giant Earth impacts.

[39] Thickened crust, for example, plainly underlies the Earth's volcanic provinces [e.g., *Mooney et al.*, 1998; *von Frese et al.*, 1999; *Leftwich et al.*, 2005], but active tectonic and erosion processes have scrubbed much of the visible crustal impact history from the geologic record. However, some of the Earth's obscure impact history may well be recorded by the roughly 49% of its large igneous provinces and hot spots that are antipodal to each other [*Hagstrum*, 2005]. Certainly, the P-Tr antipodal relationship of the Siberian Traps to the large subglacial basin in Wilkes Land (Figure 3) on anomalously thinned and isostatically disturbed crust (Figure 4) is consistent with the effects of giant impact.

[40] Significant hot spot relationships at both the inferred Wilkes Land impact site and its antipode suggest new tectonic perspectives for these sites. For example, at ~131 Ma the impact site was within several degrees of the Kerguelen hot spot when it began forming the Kerguelen Plateau [*Coffin et al.*, 2000]. Thus, a possible consequence of the giant impact may have been the injection of

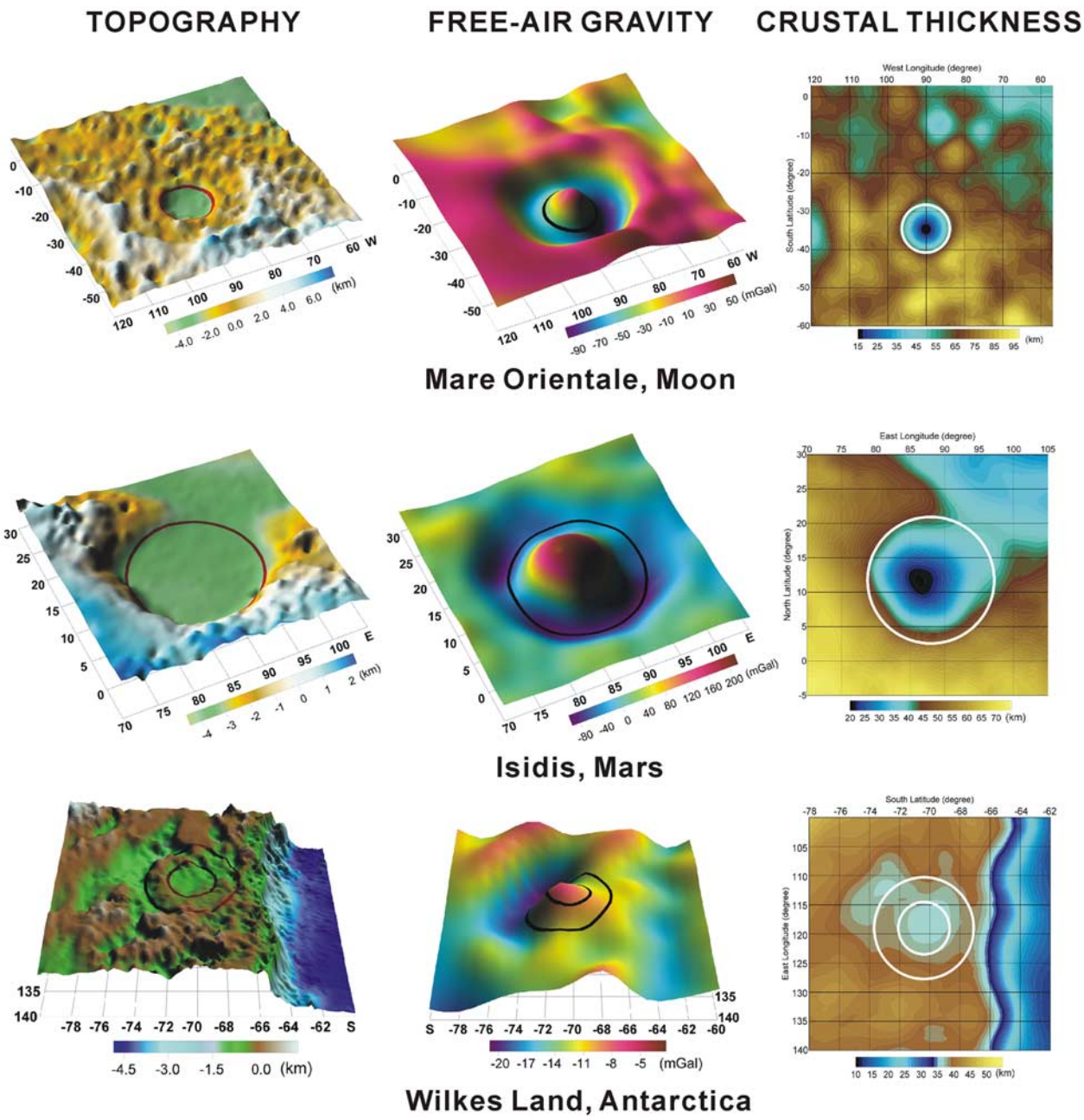

Figure 9. Generalized crustal properties for the lunar Mare Orientale basin [*von Frese et al.*, 1997], the Isidis basin of Mars [*Potts et al.*, 2004], and the Wilkes Land impact basin reveal common effects of giant meteorite impact. The lunar and Martian spherical patches list degrees latitude and longitude along the respective left and bottom axes, and vice versa for the Wilkes Land basin. The circles broadly outline the topographic boundaries of the central basins.

considerable thermal energy and fracturing into the crust and mantle that promoted the development of the hot spot and related rifting of Australia from India and East Antarctica.

[41] However, the Wilkes Land impact probably occurred much earlier with the onset of the greatest known mass extinction in the history of life near the end of the Permian. The bimodal P-Tr extinction event may reflect the initial toxic effects of enormous impact at ~260 Ma and the subsequent antipodal development of flood basalt volcanism at the Siberian Traps, which contributed significantly to the great mass extinction [e.g., *Renne and Basu*, 1991]. Plate tectonic reconstructions and mafic intrusive complexes that were emplaced in the high Arctic in the Mesozoic appear to track the Iceland hot spot back to the Siberian Traps [*Lawver and Müller*, 1994; *Lawver et al.*, 2002]. Thus, our

estimate for the date of the Wilkes Land impact implies that its antipodal effects may be related to the development of the Siberian Traps and perhaps the Iceland hot spot.

[42] However, this inference is provisional because of our limited understanding of energy transfer from giant impacts to their antipodes [e.g., *Boslough et al.*, 1996]. Additionally, the evolution of the Iceland hot spot is poorly understood with some studies suggesting that it first emerged at ~55 Ma under Greenland [e.g., *White and McKenzie*, 1989; *Sleep*, 1997], and others indicating that it developed much earlier [e.g., *Braun et al.*, 2007, and references therein].

[43] Our analysis involves extensive data sets for Antarctica that include nearly 2 million ice thickness measurements and over 11 million line kilometers of GRACE gravity observations. Figure 9 summarizes our arguments for the impact origins of the Wilkes Land basin in terms of the comparable crustal properties of the lunar and Martian impact basins of Mare Orientale [*von Frese et al.*, 1997; *Potts and von Frese*, 2003a, 2003b] and Isidis [*Potts et al.*, 2004], respectively. These basins all involve depressed terrains (Figure 9, left) with gravity effects that are consistent with underlying thinned crust (Figure 9, right) and overlain at satellite altitude by circular free-air anomaly maxima flanked by negative anomaly rings (Figure 9, middle).

[44] Furthermore, the P-Tr antipodal relationship between the Wilkes Land crater and the Siberian Traps accords with the inferred impact being older than ~100 Ma when the coastline presumably developed across the basin rings. These results, however, are not unique due to data and modeling errors and the fundamental source ambiguity of gravity analysis. Thus, their use clearly requires care and additional geological and geophysical testing.

4. Conclusions

[45] Evidence for a giant impact in north central Wilkes Land of East Antarctica is indicated by a well-defined GRACE free-air gravity maximum with flanking negative ring anomaly that overlies a huge 500-km diameter subglacial depression. The crater's terrain gravity effects may be modeled by an underlying roughly 425-km wide, 5-km thick mantle plug produced by crustal rebound from meteorite impact. However, the inferred mascon signal in the GRACE gravity data suggests that only about 90% of the mantle plug's mass may be isostatically compensated at the Moho. Excess crust around the margin of the crater can account for the negative anomalies flanking the central gravity maximum.

[46] The giant impact helps to account for the extensively disrupted and thinned Wilkes Land crust relative to the enigmatic lack of crustal thinning on the conjugate Australian block. The coastline appears to cut across the crustal rings of the inferred Wilkes Land impact crater, and thus the impact may have predated and perhaps influenced the development of the Kerguelen hot spot and the Cretaceous rifting of India and Australia from East Antarctica.

[47] Micrometeorite evidence in the Permian-Triassic boundary beds of Graphite Peak may relate the impact to the greatest mass extinction of life on Earth and the antipodal Siberian Traps. The fossil record suggests that the extinction occurred from about 260 to 250 Ma so that the impact presumably would have initiated the event. By this scenario, the impact produced the crater and extensively disrupted and thinned the Wilkes Land crust at ~260 Ma and either caused or significantly energized the great volcanic eruptions of the Siberian Traps near the end of the extinction period. Thus, the environmentally toxic effects of the impact may have played out over a period of about 10 million years.

[48] The fact that impacts produce antipodal effects is clear from studies of the lunar and Martian basins and the observation that essentially half of the Earth's large igneous provinces and hot spots are antipodal to each other. However, the processes by which great impacts produce antipodal effects are poorly understood and controversial at present.

[49] For the past 30–40 million years, direct geological evidence of the crater has been under glacial ice up to 2–3 km thick [e.g., *Ingólfson*, 2004]. However, the inferred mascon and flanking excess crust should yield detectable signals like the prominent airborne gravity effects computed in Figure 5c. Thus, surveying the prospective crater for related airborne gravity and magnetic anomalies is perhaps the most expedient and viable test of its impact origins.

Acknowledgments

[50] The Office of Polar Programs of the U.S. National Science Foundation under research grant NSF-OPP 0338005, the Ohio Supercomputer Center at Ohio State University, and the Goddard Earth Sciences and Technology Center Research Fellowship awarded to HRK supported elements of this

research. We thank two anonymous reviewers for their constructive comments.

References

Barlow, N. G. (1990), Constraints on early events in Martian history as derived from the cratering record, *J. Geophys. Res.*, *95*, 14,191–14,201, doi:10.1029/JB095iB09p14191.

Basu, A. R., M. I. Petaev, R. J. Poreda, S. B. Jacobsen, and L. Becker (2003), Chondritic meteorite fragments associated with the Permian-Triassic boundary in Antarctica, *Science*, *302*, 1388–1392, doi:10.1126/science.1090852.

Becker, L., R. J. Poreda, A. R. Basu, K. O. Pope, T. M. Harrison, C. Nicholson, and R. Iasky (2004), Bedout: A possible end-Permian impact crater offshore of northwestern Australia, *Science*, *304*, 1469–1476, doi:10.1126/science.1093925.

Bell, R. E., C. Small, and R. A. Arko (2002), Development of a new generation gravity map of Antarctica: ADGRAV Antarctic Digital Gravity Synthesis, *Ann. Geofis.*, *42*, 261–270.

Boslough, M. B., E. P. Chael, T. G. Trucano, D. A. Crawford, and D. L. Campbell (1996), Axial focusing of impact energy in the Earth's interior: A possible link to flood basalts and hotspots, in *The Cretaceous-Tertiary Event and Other Catastrophes in Earth History*, edited by G. Ryder, D. Fastovsky, and A. Gartner, *Geol. Soc. of Am. Spec. Pap.*, *307*, 541–550.

Braun, A., H. R. Kim, B. Csathó, and R. R. B. von Frese (2007), Gravity-inferred crustal thickness of Greenland, *Earth Planet. Sci. Lett.*, *262*, 138–158, doi:10.1016/j.epsl.2007.07.050.

Carporzen, L., S. A. Glider, and R. J. Hart (2005), Paleomagnetism of the Vredefort meteorite crater and implications for craters on Mars, *Nature*, *435*, 198–201.

Clitheroe, G., O. Gudmundsson, and B. L. N. Kennett (2000), The crustal thickness of Australia, *J. Geophys. Res.*, *105*, 13,697–13,714, doi:10.1029/1999JB900317.

Coffin, M. F., et al. (2000), Leg 183 Summary: Kerguelen Plateau-Broken Ridge-A large igneous province, *Proc. Ocean Drill. Program Init. Rep.*, *183*, 1–101. (Available at www-odp.tamu.edu/publications/183_IR/183ir.htm)

Collinson, J. W., W. R. Hammer, R. A. Askin, and D. H. Elliot (2006), Permian-Triassic boundary in the central Transantarctic Mountains, Antarctica, *Geol. Soc. Am. Bull.*, *118*, 747–763, doi:10.1130/B25739.1.

Daily, W., and P. Dyal (1979), Theories for the formation of lunar magnetism, *Phys. Earth Planet. Inter.*, *20*, 255–270, doi:10.1016/0031-9201(79)90049-9.

Drewry, D. J. (1983a), The bedrock surface of Antarctica, in *Antarctica: Glaciological and Geophysical Folio*, scale 1:6000000, sheet 3, edited by D. J. Drewry and S. R. Jordan, Scott Polar Res. Inst., Cambridge Univ., Cambridge, U.K.

Drewry, D. J. (1983b), Isostatically adjusted bedrock surface of Antarctica, in *Antarctica: Glaciological and Geophysical Folio*, scale 1:10000,000, sheet 6, edited by D. J. Drewry and S. R. Jordan, Scott Polar Res. Inst., Cambridge Univ., Cambridge, U.K.

Erwin, D. H. (1994), The Permo-Triassic extinctions, *Nature*, *367*, 231–236, doi:10.1038/367231a0.

Hagstrum, J. T. (2005), Antipodal hotspots and catastrophes: Were oceanic large-body impacts the cause?, *Earth Planet. Sci. Lett.*, *236*, 13–27, doi:10.1016/j.epsl.2005.02.020.

Hartmann, W. K. (1999), Martian cratering VI: Crater count isochrons and evidence for recent volcanism from Mars Global Surveyor, *Meteorit. Planet. Sci.*, *34*, 167–177.

Hartmann, W. K., and D. C. Berman (2000), Elysium Planitia lava flows: Crater count chronology and geological implications, *J. Geophys. Res.*, *105*, 15,011–15,025, doi:10.1029/1999JE001189.

Hartmann, W. K., J. Anguita, M. A. de la Casa, D. C. Berman, and E. V. Ryan (2001), Martian cratering 7: The role of impact gardening, *Icarus*, *149*, 37–53, doi:10.1006/icar.2000.6532.

Ingólfson, Ó. (2004), Quaternary glacial and climate history of Antarctica, in *Quaternary Glaciations–Extent and Chronology*, part III, edited by J. Ehlers and P. L. Gibbard, pp. 3–43, Elsevier, New York.

Isozaki, Y. (2004), Stratigraphy of the middle-upper Permian and lower-most Triassic at Chaotian, Sichuan, China, *Proc. Jpn. Acad., Ser. B*, *80*, 10–16, doi:10.2183/pjab.80.10.

Ivanov, B. A., and H. J. Melosh (2003), Large scale impacts and triggered volcanism, paper presented at Third International Conference on Large Meteorite Impacts, Lunar and Planet. Inst., Nördlingen, Germany. (Available at http://www.lpi.usra.edu/meetings/largeimpacts2003/pdf/4062.pdf)

Jones, A. P., G. D. Price, N. J. Price, P. S. DeCarli, and R. A. Clegg (2002), Impact induced melting and the development of large igneous provinces, *Earth Planet. Sci. Lett.*, *202*, 551–561, doi:10.1016/S0012-821X(02)00824-5.

Lawver, L. A., and R. D. Müller (1994), The Iceland hotspot track, *Geology*, *22*, 311–314, doi:10.1130/0091-7613(1994)022<0311:IHT>2.3.CO;2.

Lawver, L. A., A. Grantz, and L. M. Gahagan (2002), Plate kinematic evolution of the present arctic region since the Ordovician, in *Tectonic Evolution of the Bering Shelf-Chukchi Sea-Arctic Margin and Adjacent Landmasses*, edited by E. L. Miller, A. Grantz, and S. L. Klemperer, *Geol. Soc. Am. Spec. Pap.*, *300*, 333–358.

Leftwich, T. E. (2006), Geophysical investigations of the crustal structure and evolution of Mars, 203 pp., Ph.D. dissertation, Dept. of Geol. Sci., Ohio State Univ., Columbus.

Leftwich, T. E., R. R. B. von Frese, L. V. Potts, H. R. Kim, D. R. Roman, P. T. Taylor, and M. Barton (2005), Crustal modeling of the North Atlantic from spectrally correlated free-air and terrain gravity, *J. Geodyn.*, *40*, 23–50, doi:10.1016/j.jog.2005.05.001.

Lemoine, F. G., et al. (1998), The development of the Joint NASA GSFC and National Imagery and Mapping Agency (NIMA) Geopotential Model EGM96, *NASA/TP-1998–206861*, NASA Goddard Space Flight Cent., Greenbelt, Md.

Lythe, M. B., D. G. Vaughan, and the BEDMAP Consortium (2001), BEDMAP: A new ice thickness and subglacial topographic model of Antarctica, *J. Geophys. Res.*, *106*, 11,335–11,352, doi:10.1029/2000JB900449.

Marks, K. M., and D. C. McAdoo (1992), Gravity field over the southern oceans, *NGDC Rep. MGG-6*, NOAA, Silver Spring, Md.

Melosh, H. J. (1989), *Impact Cratering: A Geologic Process*, 245 pp., Oxford Univ. Press, New York.

Melosh, H. J. (2000), Impacts do not initiate volcanic eruptions: Eruptions close to the crater, *Proc. Lunar Planet. Sci. Conf.*, *XXXIV*, 1338.

Melosh, H. J. (2003a), Can impacts induce volcanic eruptions?, *Proc. Lunar Planet. Sci. Conf.*, *XXXVII*, 3144.

Melosh, H. J. (2003b), Modeling meteorite impacts: What we know and what we would like to know, *Proc. Lunar Planet. Sci. Conf.*, *XXXVII*, 8053.

Mooney, W., G. Laske, and T. Masters (1998), Crust 5.1: A global crustal model at 5° × 5°, *J. Geophys. Res.*, *103*, 727–747, doi:10.1029/97JB02122.

Muller, P. M., and W. L. Sjogren (1968), Mascons: Lunar mass concentrations, *Science*, *161*, 680–684, doi:10.1126/science.161.3842.680.

Müller, R. D., A. Goncharov, and A. Kritski (2005), Geophysical evaluation of the enigmatic Bedout basement high, offshore northwestern Australia, *Earth Planet. Sci. Lett.*, *237*, 264–284, doi:10.1016/j.epsl.2005.06.014.

Neumann, G. A., M. T. Zuber, M. A. Wieczorek, P. J. McGovern, F. G. Lemoine, and D. E. Smith (2004), Crustal structure of Mars from gravity and topography, *J. Geophys. Res.*, *109*, E08002, doi:10.1029/2004JE002262.

Penfield, G. T., and A. Camargo-Zanoguera (1981), Definition of a major igneous zone in the central Yucatán platform with aeromagnetics and gravity, 51st Annual Meeting, Soc. of Explor. Geophys., Tulsa, Okla.

Poreda, R. J., and L. Becker (2003), Fullerenes and interplanetary dust at the Permian-Triassic boundary, *Astrobiology*, *3*, 75–90, doi:10.1089/153110703321632435.

Potts, L. V., and R. R. B. von Frese (2003a), Comprehensive mass modeling of the Moon from spectrally correlated free-air and terrain gravity data, *J. Geophys. Res.*, *108*(E4), 5024, doi:10.1029/2000JE001440.

Potts, L. V., and R. R. B. von Frese (2003b), Crustal attributes of lunar basins from terrain-correlated free-air gravity anomalies, *J. Geophys. Res.*, *108*(E5), 5037, doi:10.1029/2000JE001446.

Potts, L. V., and R. R. B. von Frese (2005), Impact-induced mass flow effects on lunar shape and the elevation dependence of nearside maria with longitude, *Phys. Earth Planet. Inter.*, *153*, 165–174, doi:10.1016/j.pepi.2005.06.013.

Potts, L. V., R. R. B. von Frese, T. E. Leftwich, P. T. Taylor, C. K. Shum, and R. Li (2004), Gravity-inferred crustal attributes of visible and buried impact basins on Mars, *J. Geophys. Res.*, *109*, E09009, doi:10.1029/2003JE002225.

Press, F., and G. Dewart (1959), Extent of the Antarctic Continent, *Science*, *129*, 462–463, doi:10.1126/science.129.3347.462.

Reese, C. C., V. S. Solomatov, and J. R. Baumgardner (2002), Survival of impact-induced thermal anomalies in the Martian mantle, *J. Geophys. Res.*, *107*(E10), 5082, doi:10.1029/2000JE001474.

Renne, P. R., and A. R. Basu (1991), Rapid eruption of the Siberian Traps flood basalts at the Permo-Triassic Boundary, *Science*, *253*, 176–179, doi:10.1126/science.253.5016.176.

Retallack, G. J., A. Seyedolali, E. S. Krull, W. T. Hoiser, C. P. Ambers, and F. T. Kyte (1998), Search for evidence of impact and the Permian-Triassic boundary in Antarctica and Australia, *Geology*, *26*, 979–982, doi:10.1130/0091-7613(1998)026<0979:SFEOIA>2.3.CO;2.

Richmond, N. C., L. L. Hood, D. L. Mitchell, R. P. Lin, M. H. Acuña, and A. B. Binder (2005), Correlations between magnetic anomalies and surface geology antipodal to lunar impact basins, *J. Geophys. Res.*, *110*, E05011, doi:10.1029/2005JE002405.

Ritzwoller, M. H., N. M. Shapiro, A. L. Levshin, and G. M. Leahy (2001), Crustal and upper mantle structure beneath Antarctica and surrounding oceans, *J. Geophys. Res.*, *106*, 30,645–30,670, doi:10.1029/2001JB000179.

Schultz, P. H. (2007), A possible link between Porcellarum and the South-Pole-Aitken Basin, *Proc. Lunar Planet. Sci. Conf.*, *XXXVIII*, 1839.

Schultz, P. H., and D. E. Gault (1975), Seismic effects from major basin formation on the Moon and Mercury, *Moon*, *12*, 159–177, doi:10.1007/BF00577875.

Schultz, P. H., and H. Glicken (1979), Impact crater and basin control of igneous processes on Mars, *J. Geophys. Res.*, *84*, 8033–8047, doi:10.1029/JB084iB14p08033.

Siegert, M. J. (2000), Antarctic subglacial lakes, *Earth Sci. Rev.*, *50*, 29–51, doi:10.1016/S0012-8252(99)00068-9.

Sleep, N. H. (1997), Lateral flow and ponding of starting plume material, *J. Geophys. Res.*, *102*, 10,001–10,012, doi:10.1029/97JB00551.

Smith, A. G., A. M. Hurley, and J. C. Briden (1981), *Phanerozoic Paleocontinental World Maps*, *Cambridge Earth Sci. Ser.*, 102 pp., Cambridge Univ. Press, London.

Smith, D. E., et al. (1999a), The global topography of Mars and implications for surface evolution, *Science*, *284*, 1495–1530, doi:10.1126/science.284.5419.1495.

Smith, D. E., W. L. Sjogren, G. L. Tyler, G. Balmino, F. G. Lemoine, and A. S. Konopliv (1999b), The gravity field of Mars: Results from the Mars Global Surveyor, *Science*, *286*, 94–97, doi:10.1126/science.286.5437.94.

Spudis, P. D. (2005), *The Geology of Multi-Ring Impact Basins*, 277 pp., Cambridge Univ. Press, New York.

Stampfli, G. M., and G. D. Borel (2002), A plate tectonic model for the Paleozoic and Mesozoic constrained by dynamic plate boundaries and restored synthetic oceanic isochrons, *Earth Planet. Sci. Lett.*, *196*, 17–33, doi:10.1016/S0012-821X(01)00588-X.

Stanley, S. M., and X. Yang (1994), A double mass extinction at the end of the Paleozoic Era, *Science*, *266*(5189), 1340–1344, doi:10.1126/science.266.5189.1340.

Tapley, B. D., S. Bettadpur, M. Watkins, and C. Reigber (2004), The gravity recovery and climate experiment; Mission overview and early results, *Geophys. Res. Lett.*, *31*, L09607, doi:10.1029/2004GL019920.

von Frese, R. R. B., W. J. Hinze, L. W. Braile, and A. J. Luca (1981), Spherical earth gravity and magnetic anomaly modeling by Gauss-Legendre quadrature integration, *J. Geophys.*, *49*, 234–242.

von Frese, R. R. B., L. Tan, L. V. Potts, C. J. Merry, and J. D. Bossler (1997), Lunar crustal analysis of Mare Orientale from topographic and gravity correlations, *J. Geophys. Res.*, *102*, 25,657–25,675, doi:10.1029/97JE02216.

von Frese, R. R. B., L. Tan, J. W. Kim, and C. R. Bentley (1999), Antarctic crustal modeling from the spectral correlation of free-air gravity anomalies with the terrain, *J. Geophys. Res.*, *104*, 25,275–25,296, doi:10.1029/1999JB900232.

von Frese, R. R. B., H. R. Kim, P. T. Taylor, and M. F. Asgharzadeh (2005), Reliability of CHAMP anomaly continuations, in *Earth Observation with CHAMP*, edited by C. Reigber, H. Lühr, and J. Wickert, pp. 287–292, Springer, Berlin.

Watts, A. W., R. Greeley, and H. J. Melosh (1991), The formation of terrains antipodal to major impact basins, *Icarus*, *93*, 159–168, doi:10.1016/0019-1035(91)90170-X.

Wells, S. B. (2006), Regional geophysical analysis of the Antarctic lithosphere and investigation of the proposed Wilkes Land impact crater, M.Sc. thesis, Ohio State Univ., Columbus.

White, R. S., and D. McKenzie (1989), Magmatism at rift zones: The generation of volcanic continental margins and flood basalts, *J. Geophys. Res.*, *94*, 7685–7729, doi:10.1029/JB094iB06p07685.

Williams, D. A., and R. Greeley (1994), Assessment of antipodal impact terrains on Mars, *Icarus*, *110*, 196–202, doi:10.1006/icar.1994.1116.

Wise, D. U., and M. T. Yates (1970), Mascons as structural relief on a lunar Moho, *J. Geophys. Res.*, *75*, 261–268, doi:10.1029/JB075i002p00261.